



Ultrasonic-enhanced selective sulfide precipitation of copper ions from copper smelting dust using monoclinic pyrrhotite

Xing-fei ZHANG^{1,2}, Jia YUAN^{1,2}, Jia TIAN^{1,2}, Hai-sheng HAN^{1,2},
Wei SUN^{1,2}, Tong YUE^{1,2}, Yue YANG^{1,2}, Li WANG^{1,2}, Xue-feng CAO^{1,2}, Cheng-long LU^{1,2}

1. School of Minerals Processing and Bioengineering, Central South University, Changsha 410083, China;
2. Key Laboratory of Hunan Province for Clean and Efficient Utilization of Strategic Calcium-containing Mineral Resources, Central South University, Changsha 410083, China

Received 11 January 2021; accepted 8 September 2021

Abstract: The sulfide passivation film produced on the surface seriously prevents further reaction in the process of using monoclinic pyrrhotite (MPr) to treat heavy metal ions in wastewater. Ultrasonic technology was introduced to assist MPr to recover the copper ions. XPS result proves that CuS products exist on the surface of MPr. XRD and SEM results show that the CuS on the particles' surface is stripped under ultrasonic condition. The kinetics results indicate that the reaction under both conventional and ultrasonic conditions conform to the Avrami model. The reaction process changes from diffusion control to chemical reaction control under the ultrasonic condition as the solid layer is stripped off. The presence of ultrasonic significantly reduces the acidity and temperature required for the reaction and enhances the utilization efficiency of MPr; by controlling the amount of MPr, the removal rates of copper and arsenic in copper smelting dust leachate exceed 99% and 95%, respectively.

Key words: ultrasonic-assisted treatment; monoclinic pyrrhotite; copper smelting dust; arsenic removal; selective sulfide precipitation

1 Introduction

A large amount of copper smelting arsenic-containing dust is produced during the process of copper pyrometallurgy. In addition to the hazardous element As, the dust also contains large amounts of recoverable valuable metals such as Cu, Pb, and Zn. At present, most plants return the dust directly to the smelting system for treatment, resulting in arsenic circulation and accumulation in the smelting system, which not only causes harm to workers' health but also seriously deteriorates the quality of products [1,2]. In contrast, wet processing shows more significant advantages [3,4]. The H₂SO₄ leaching allows valuable metals and arsenic in the dust to enter the solution. Then, the selective

cascade separation of polymetallic elements helps realize the resource utilization of valuable metals and the safe treatment of arsenic [5].

Currently, the most widely used method is to add a sulfurizing agent into the leachate to precipitate the ions according to their solubility products. However, the most commonly used reagents in industry, Na₂S and NaHS, have many shortcomings: (1) low purification and separation efficiency; (2) a large amount of H₂S gas is easily generated during the reaction [6]; (3) the product has a fine particle size and is difficult to filter. Therefore, new sulfurizing agents that can overcome or alleviate these shortcomings are urgently needed.

Our previous study [7] showed that the synthetic monoclinic pyrrhotite (MPr) can act as a

cheap and clean S^{2-} sustained-release reagent to precipitate most metal ions in the wastewater, avoiding the introduction of Na^+ harmful to industrial production and the escape of H_2S . However, the sulfide passivation film produced on the surface seriously prevents further reaction. YANG et al [8] found that the surface of FeS is wholly overlaid by the precipitated CuS during processing the wastewater containing copper ions, which reduces the dissolution of pyrrhotite and further reactions.

In the past few decades, a new technology named ultrasonic-assisted leaching for ore dressing has been widely used in hydrometallurgy [9,10]. It has the characteristics of high power, short wavelength, and high frequency. The promotion of the liquid reaction process is mainly due to the “acoustic cavitation” phenomenon produced by ultrasonic waves in the solution [11–13]. BRUNELLI and DABALA [14] performed an ultrasonic-assisted leaching process to recover zinc from an electric arc furnace (EAF). The results showed that the ultrasound irradiation led to a 55% increase in the Zn leaching compared to conventional conditions. LI et al [15] prepared the high purity nickel sulfate assisted by ultrasonic. The ultrasonic treatment can peel off oxide film on the nickel’s surface to increase the leaching quantity of nickel sulfate. ZHANG et al [16] found that ultrasonic agitation can effectively reduce energy consumption and decrease acid concentration. The copper removal behavior of MPr can be regarded as the leaching of pyrrhotite in the copper sulfate solution. Therefore, it is possible to use ultrasonic technology as an auxiliary means to improve the utilization efficiency of MPr and optimize the conditions required for the reaction.

In this work, ultrasonic wave was introduced as the outfield enhanced method to improve the utilization efficiency of MPr. The influence parameters such as the ultrasonic power intensity, acid concentration, reaction temperature, and time of copper ion removal with MPr were assessed. XRD, XPS, and SEM analyses were performed to deeply reveal the enhancement mechanism in removing copper ions by MPr. Meanwhile, the reaction kinetics was studied to compare the reaction-controlled types of conventional and ultrasonic conditions. This work aims to provide a method for the industrial application of MPr in

polymetallic acid wastewater in the future.

2 Experimental

2.1 Materials

The MPr used in the experiment was prepared by self-synthesis, and the preparation and classification methods are the same as the previous study [7]. The elements content and surface morphology of the new synthetic MPr are present in Table S1 and Fig. S1 in Supplementary Information (SI), respectively. The water samples treated in the experiment were divided into self-prepared simulated copper solution and actual copper smelter dust leaching solution. The simulated copper solution was used to study the kinetics and mechanism of copper removal with MPr. The dosage of copper sulfate pentahydrate and sulfuric acid were calculated, and then the required concentration and acidity of the simulated copper solutions were prepared for use. Copper sulfate pentahydrate ($CuSO_4 \cdot 5H_2O$, supplied by Shanghai Aladdin Bio-chem Technology Co., Ltd.) and sulfuric acid (98%, mass fraction) were used to prepare a simulation solution with the required copper ion concentration and acidity for use; the raw materials used in the actual leachate were taken from the copper smelter dust produced by Western Mining Co., Ltd., Qinghai, China. The original dust characterization shows that there are many kinds of elements and minerals, the relationship between minerals is complicated and the particles are extremely fine (Table S2, Figs. S2, and S3 in SI).

2.2 Experimental procedure

2.2.1 Leaching experiment

A series of leaching experiments were carried out to explore the influence of various factors (H_2SO_4 concentration, leaching time, temperature, liquid/solid ratio) on the leaching of elements in copper smelter dust. The results are shown in Fig. S4 in SI. The phase of the leached residual is mainly lead sulfate (Fig. S5 in SI), and the process stability experiment was also performed (Table S3 in SI).

2.2.2 Copper removal experiment

The copper removal experiments under conventional conditions were carried out in a three-neck round-bottom flask of 500 mL immersed in a water bath thermostat (DF-101S, Gongyi

Yuhua Instrument Co., Ltd., Gongyi, China). The stirring method adopted mechanical stirring, and a condenser was used to prevent the evaporation and loss of water under high temperatures. The experiments under ultrasonic conditions were conducted in a 500 mL beaker. The ultrasonic probe (JM-1003) was placed in the solution during the reaction, and the ultrasonic generator was purchased from Shenzhen Jiemeng Cleaning Equipment Co., Ltd., China. In each test, 200 mL of the reaction solution and a certain dosage of MPr were added to the reaction vessel and reacted at the required time and temperatures. On completion of the experiment, the solution and residue were separated. The schematic diagram is shown in Fig. 1.

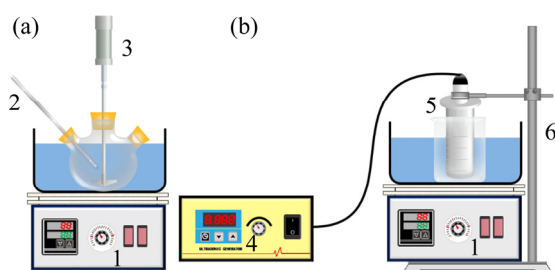


Fig. 1 Schematic diagram of conventional (a) and ultrasonic (b) conditions: 1—Water bath thermostat; 2—Thermometer; 3—Mechanical agitator; 4—Ultrasonic generator; 5—Ultrasonic probe; 6—Ring stand

2.2.3 Kinetic experiment

In the kinetic experiment, the reaction conditions were set as follows: H_2SO_4 concentration 50 g/L, MPr dosage 2 (molar ratio of S to Cu), reaction time 30 min, ultrasonic power 60 W (only in ultrasonic condition), and reaction temperatures (25, 40, 50 and 60 °C). 3 mL of the reaction solution was taken out by a pipette at the desired time both in conventional and ultrasonic conditions during the reaction. Then, 0.2 μm PTEE membranes were used to get the filtrates for analysis, while 3 mL of the initial solution was supplemented into the reaction system.

2.2.4 Calculation of elements removal rate

The solution after the reaction was filtered using a circulating water vacuum pump (SHZ-D(III), Shanghai Lunlun Instrument and Equipment Co., Ltd., China) and washed with distilled water. The concentration of ions in the filtrate was determined by ICP-AES to calculate the

ion removal rate (η_1) according to Eq. (1). The total iron ion leaching rate (η_2) was calculated according to Eq. (2):

$$\eta_1 = \frac{c_1 V_1}{c_0 V_0} \times 100\% \quad (1)$$

$$\eta_2 = \frac{c_1 V_1}{m_0 w_0} \times 100\% \quad (2)$$

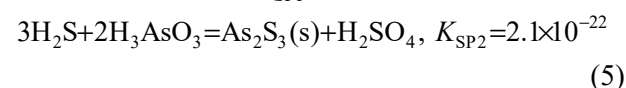
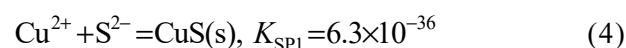
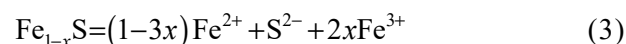
where c_1 and c_0 are the concentrations of the ions of the filtrate solution and original solution (mg/L), respectively; V_1 and V_0 are the volumes of the filtrate solution and original solution, respectively (L); m_0 represents the mass of the raw solid sample put into solution (g); w_0 represents the iron content in the raw sample (%).

2.2.5 Analytical techniques

The concentrations of copper and arsenic were determined by ICP-AES (AVIO 500, PerkinElmer, USA). The chemical component, crystal structure, surface morphologies, and elemental valence of copper removal products under different conditions were characterized by XRF (S4 Pioneer, Bruker, Germany), XRD (SIEMENS D500, Bruker, Germany), SEM (JSM-7900F, JEOL, Japan) and XPS (ESCALAB250Xi, ThermoFisher-VG Scientific, USA).

3 Results and discussion

Previous studies show that the use of MPr in copper removal from arsenic-containing wastewater shall be carried out under the condition of high temperature and strong acid. According to the principle of sulfide solubility product, copper ions can preferentially form sulfide precipitate to achieve selective separation. The mechanism of removal can be expressed by the following reactions [17]:



As shown in Fig. S6 in SI, the temperature has a significant influence on the utilization efficiency of MPr and the removal rate of copper under conventional conditions. Under low temperature conditions, the decomposition rate of MPr is slow, and the slowly generated sulfide ions will

preferentially react with copper ions to form copper sulfide and coat on the surface of MPr, making it difficult for the reaction to continue. The high temperature will accelerate the decomposition rate of MPr, and a large number of sulfide ions generated instantaneously will form copper sulfide precipitate with copper ions to improve the removal rate of copper ions, but hydrogen sulfide is generated more easily due to the competitive behavior of a large number of hydrogen ions in the solution.

To further find out the substance form and element valence state of the MPr surface product after the reaction, the XPS test was carried out. Figure 2(a) shows the energy spectrum of Cu 2p on the surface of MPr after copper removal under normal conditions. It can be seen that the binding energy of the characteristic peaks of Cu 2p_{3/2} and Cu 2p_{1/2} are 932.45 and 952.23 eV, respectively, which confirms that the copper element on the surface of the MPr after the reaction exists in the form of copper sulfide [18].

Peak fitting of S 2p was carried out to explore

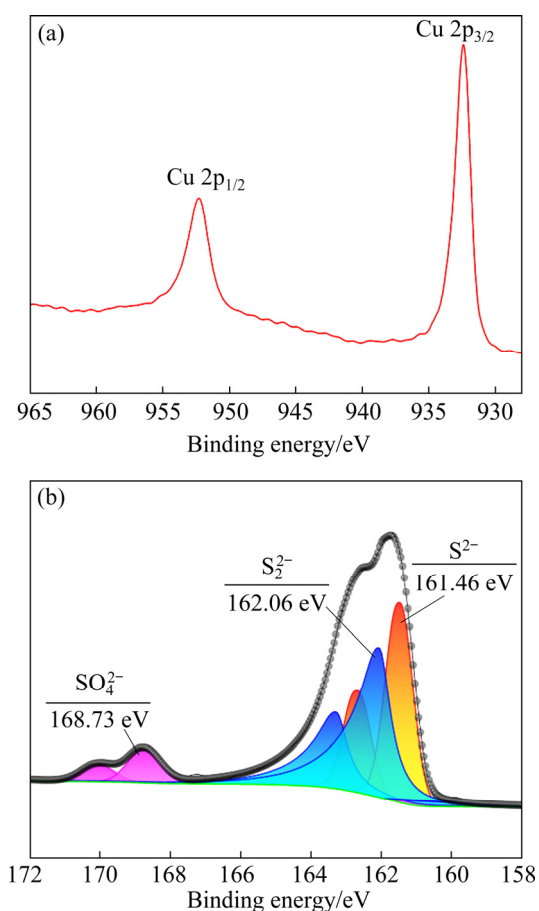


Fig. 2 XPS narrow-spectrum of Cu 2p (a), and peak fitting diagram of S 2p (b) after copper removal by MPr

the composition and valence distribution of S element on the surface of MPr after the reaction. As can be seen from Fig. 2(b), S 2p is divided into three-double peaks. The binding energies of S 2P_{2/3} are 161.46, 162.06, and 168.73 eV, which are very close to the values of 161.4 eV for monosulfide in Cu₅FeS₄ [19,20], 161.9 eV for disulfide in CuFeS₂ [21] and 168.6 eV for sulfate [22], respectively. Therefore, it can be inferred that S in the surface product after copper removal exists in the form of monosulfide and disulfide and is combined with copper and iron in the form of Cu—S—Fe. The sulfate may be caused by the oxidation of sulfide or sulfate impurities carried from the sulfuric acid solution.

Here, we still took the simulated copper sulfate solution as the research object to explore the kinetic factors that affect the removal of copper ions enhanced by ultrasonic and mechanism.

3.1 Effect of ultrasonic power on copper ion removal rate with MPr

The effect of ultrasonic power was assessed at different ultrasonic powers from 0 to 150 W with the addition of 50 g/L H₂SO₄, MPr dosage of 2 (molar ratio of S to Cu²⁺), reaction time of 30 min and reaction temperature of 25 °C.

The effect of ultrasonic power on copper ion removal rate with MPr is shown in Fig. 3. The copper ion removal rate is only 15.3% without ultrasonic, and it increases dramatically to 74.4% when the ultrasonic power is 30 W. The copper ion removal rate rises as the power increases and achieves the maximal value, 99.5%, at 150 W. This phenomenon is mainly attributed to a series of

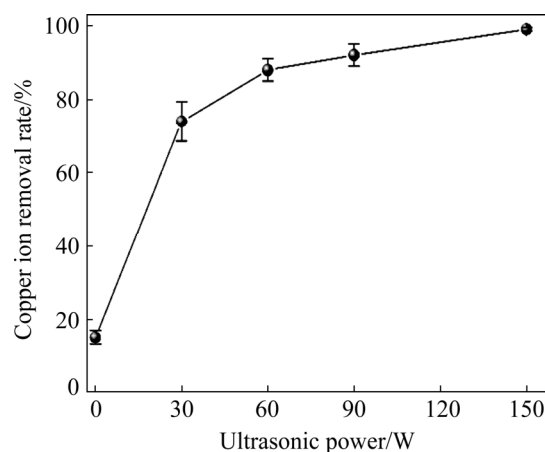


Fig. 3 Effect of ultrasonic power on copper ion removal rate with MPr

effects caused by ultrasound, such as cavitation and micro-jets [23]. The instantaneous collapse of bubbles generated by cavitation will cause local high temperatures, high pressure, and high-speed micro-jet effects. Cavitation is enhanced with the increase of ultrasonic power, so the copper removal is also enhanced. ZHANG et al [13] have shown that ultrasonic mainly affects chemical reaction at high frequency and produces mechanical effects at low frequency. The highest power of ultrasonic in this study is only 150 W, so, the effect of the ultrasonic strengthening process should mainly be the latter, consistent with the previous analysis.

3.2 Effect of H₂SO₄ concentration on copper ion removal rate with MPr

The effect of H₂SO₄ concentration was assessed at H₂SO₄ concentration from 10 to 100 g/L at ultrasonic power of 60 W, MPr dosage of 2, reaction time of 30 min, and reaction temperature of 25 °C.

As shown in Fig. 4, the copper ion removal rate increases significantly with the increase of the original H₂SO₄ concentration of the solution, indicating that the solution's acidity still played an essential role in the copper ion removal even under ultrasonic conditions. Increasing the H₂SO₄ concentration can increase the initial decomposition rate of MPr on the one hand. On the other hand, it can accelerate the mass transfer and diffusion of H⁺ and promote H⁺ to pass through the product layer under ultrasound to react with unreacted particles, thereby increasing the copper ion removal rate in the solution. However, when the concentration of H₂SO₄ is too high, it will corrode the ultrasonic

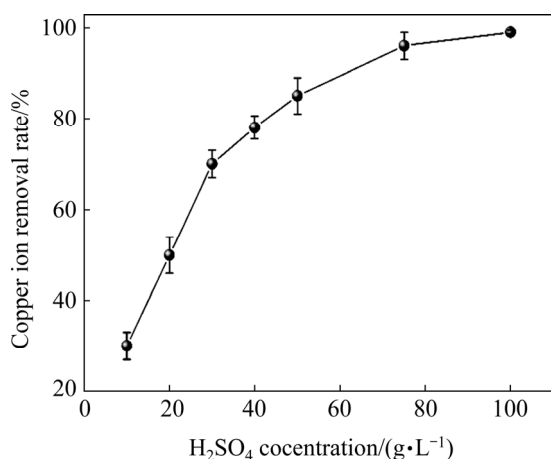


Fig. 4 Effect of H₂SO₄ concentration on copper ion removal rate with MPr at ultrasonic power of 60 W

equipment and lead to a large amount of H₂S overflowing, causing potential damage to people's health. At 50 g/L of H₂SO₄, the copper removal rate is almost the same as the copper removal under conventional conditions of 200 g/L acidity and 60 °C (Fig. S6 in SI); that is, ultrasonic can effectively reduce the required acid concentration and temperature of the reaction [16].

3.3 Effect of temperature and time on copper ion removal rate with MPr

The copper ion removal tests were carried out at different temperatures from 25 to 60 °C in 30 min with 50 g/L H₂SO₄, and MPr dosage of 2. Considering the fact that the ultrasound itself could provide energy to the system and cause temperature rise, higher power ultrasound should be avoided as much as possible to maintain a constant temperature during the reaction. Therefore, the power of ultrasound in this experiment was selected to be 60 W. The results are shown in Fig. 5.

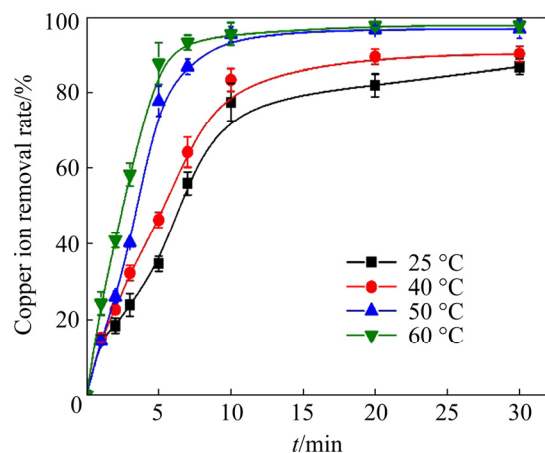


Fig. 5 Effect of temperature and time on copper ion removal rate with MPr at ultrasonic power of 60 W

The increase in temperature is also beneficial to the removal of copper ions under ultrasonic conditions. The ultrasonic treatment presented closely 100% of copper ion removal rate when the temperatures are 50–60 °C. However, ZHANG et al [13] pointed out that when the temperature is too high, the vapor pressure inside the bubble increases, which enhances the buffering effect when the bubbles collapse, and therefore weakens cavitation.

Compared with the conventional conditions (Fig. S6 in SI), under the ultrasonic conditions, the reaction does not require high temperature and high

acidity. It can also achieve or exceed the same copper ion removal rate under conventional conditions. Besides, from the perspective of the effect of time on the copper removal, the reaction process under ultrasonic conditions is controllable, and the overflow of H_2S can be significantly reduced. In a word, ultrasonic can effectively reduce energy consumption and decrease the temperature and acid concentration required for the reaction. Moreover, it improves the copper ion removal rate significantly.

To find the difference of product phase transformation in the absence and presence of ultrasonic, the XRD analysis was conducted on the products. The reaction conditions of conventional system are consistent those with the ultrasonic system (ultrasonic power of 60 W), H_2SO_4 concentration of 50 g/L, MPr dosage of 2, reaction time of 30 min, and reaction temperature of 50 °C. It can be seen in Fig. 6 that the diffraction peaks of the raw material coincide with those of FeS (PDF No. 76-0960), but the weak peak intensity indicates that it has a poor crystallinity. The new peaks of CuS (PDF No. 76-1725) appear in both conventional and ultrasonic reactants, indicating the formation of CuS in those products, but the peak intensities of CuS under ultrasonic conditions are significantly stronger than those under traditional conditions. Combined with the copper ion removal in the solution, it means that the enhancement of peak intensity is due to the high content of copper sulfide in the ultrasonic product. Also, the increase of the peak intensity of the raw material FeS after

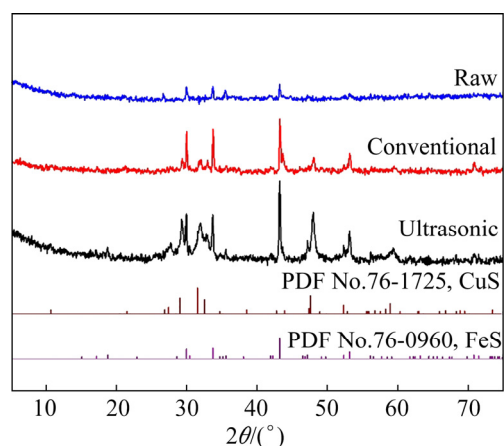


Fig. 6 XRD patterns of raw MPr and residues obtained under conventional and ultrasonic conditions

the reaction shows that its crystal structure is more stable, leading to a decrease of reactivity.

Figure 7 shows the SEM images of residues under conventional and ultrasonic conditions, revealing the difference in microstructure of reaction products. It can be found that the MPr surface is tightly wrapped by flocculent CuS under conventional conditions (Fig. 7(a)), and the flocs products are massive, existing in the form of agglomerates (Fig. 7(b)). The pores of MPr are also filled with a large amount of flocs CuS (Fig. 7(c)). The flocculent CuS highly prevents further reaction. On the contrary, under ultrasonic conditions, the CuS generated on the surface of MPr is peeled off based on the effect of cavitation and micro-jet (Fig. 7(d)). MPr re-exposes a new body and some particles develop new cracks on the surface

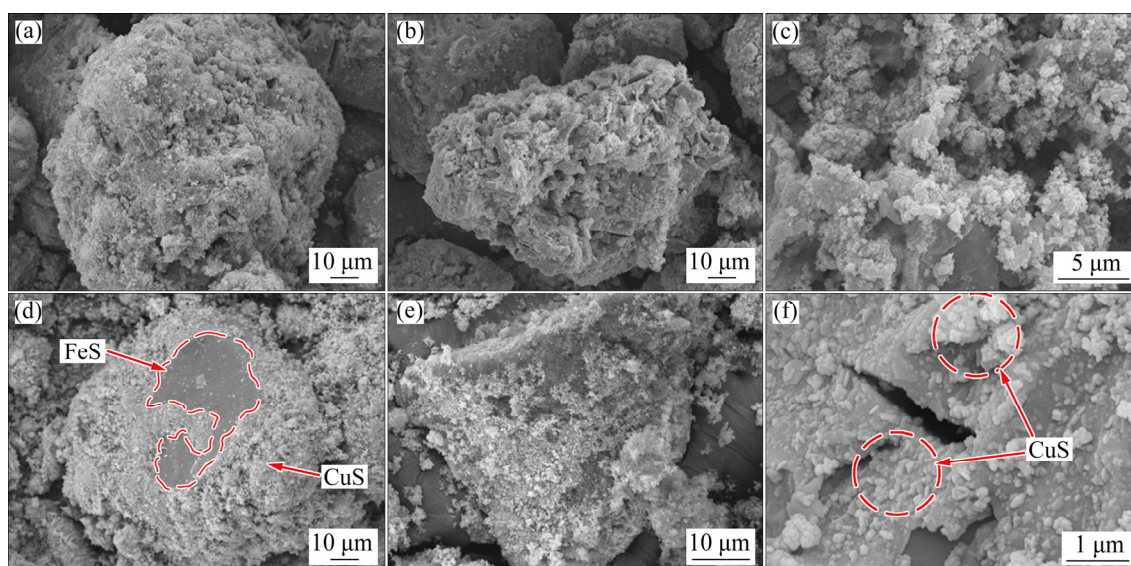


Fig. 7 SEM images of residues obtained under conventional (a–c) and ultrasonic (d–f) conditions

(Fig. 7(f)). Besides, the CuS flocculent particles are dotted, and loosely distributed around and on the surface of the MPr particles (Figs. 7(e, f)) due to the vibration and dispersion of ultrasonic waves during the formation process, which are not easy to aggregate into a deep coating on the MPr surface. These phenomena significantly reduce the reaction resistance and promote the reaction efficiency of MPr. These changes in surface morphology also demonstrate the enhanced effect of ultrasonic.

3.4 Kinetic analysis

The copper removal behavior of MPr can be regarded as the decomposition process of MPr in a strongly acidic solution, which belongs to the liquid–solid reaction process [24]. The only difference is that copper ions in the solution will form CuS, affecting the decomposition of MPr. The removal of copper ions in the solution is directly proportional to the leaching of iron ions. Therefore, the leaching of iron ions can be taken as the research object and substituted into the relevant kinetic model for analysis to clarify the main control steps in the reaction process and provide guidance for the next stage of the reaction. The leaching results of iron ions under conventional and ultrasonic conditions at different temperatures and time are shown in Fig. 8.

Firstly, a theoretical model of the unreacted shrinking core is adopted, which assumes that the reaction occurs on the solid's outer surface. As the reaction proceeds, this surface shrinks toward the solid center, leaving an inert solid layer. The macroscopic reaction process is composed of external diffusion, internal diffusion, and surface chemical reaction. The greatest resistance is the

control stage of the overall rate. For the surface chemical reaction-controlled type, there exists [25]:

$$1-(1-x)^{1/3}=k_c t \quad (6)$$

For diffusion-controlled type, there exists [26]:

$$1-3(1-x)^{2/3}+2(1-x)=k_d t \quad (7)$$

where x is the extraction fraction of iron ions, t is the reaction time, k_c is the surface chemical reaction rate constant, and k_d is the diffusion rate constant.

After the above analysis, it is assumed that the leaching process conforms to the unreacted shrinking core model. The conventional experiment results are respectively substituted into Eqs. (6) and (7) for fitting, and the reaction's control types are determined according to the correlation coefficients R^2 . Taking into account different time for the reaction to reach equilibrium at different temperatures, the data of the first 10 min are used for fitting at 25 and 40 °C, and the data of the first 5 min are used at 50 and 60 °C. The fitting results are shown in Table 1 and Fig. S7 in SI.

Table 1 shows the linear fitting between the experimental data, and the chemical reaction control model is imperfect. The correlation coefficient (R^2) only reaches 0.868 at 60 °C and does not exceed 0.8 at other temperatures, indicating that the chemical reaction does not control the reaction process. In contrast, the experimental data fit well with the diffusion control model, which means that the reaction process might be controlled by diffusion. In other words, the solid CuS film generated on the surface of MPr during the reaction process would hinder the continuation of the reaction, making the diffusion of the leaching agent the foremost control step. However, the value

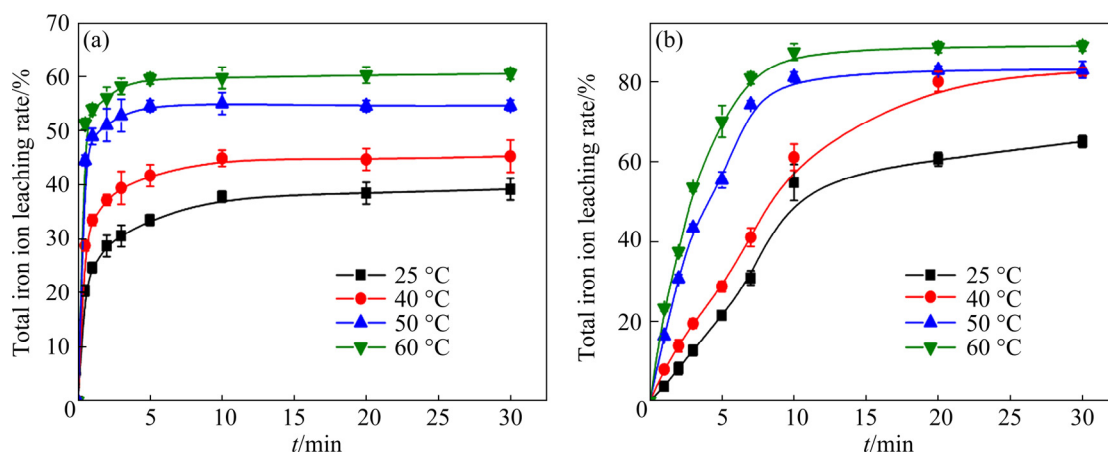


Fig. 8 Effect of temperature on total iron ion leaching rate under conventional (a) and ultrasonic (b) conditions

Table 1 Correlation coefficients (R^2) of chemical reaction control and diffusion control models at different temperatures

Temperature/ °C	Correlation coefficient (R^2)	
	$1 - (1-x)^{1/3} = k_c t$	$1 - 3(1-x)^{2/3} + 2(1-x) = k_d t$
25	0.7885	0.9094
40	0.6411	0.8624
50	0.6004	0.8441
60	0.8681	0.9134

of R^2 is generally maintained below 0.92, showing that the unreacted shrinking core model is not the ideal model, and the inert solid layer may not increase gradually from the outside to the inside.

In addition, there is also a kinetic equation that is widely used in the leaching reaction process, namely the Avrami equation [27], as shown in Eq. (8). This equation was first proposed and applied well in crystallization kinetics [28,29]. It assumes that nucleation occurs randomly and homogeneously throughout the untransformed part of the material. The growth rate does not depend on the extent of transformation, and the growth rate in all directions is the same [30]. LI et al [31] believed that the good applicability of Avrami equation in leaching reaction may be attributed to the fact that the leaching reaction can be regarded as the reverse process of the crystallization process. TIAN et al [32] used Avrami model to fit the dynamic model of arsenic leaching process from copper smelting dust. The results showed that the reaction was controlled by diffusion and the activation

energy of the reaction was 7.58 kJ/mol. HE et al [33] and SHI et al [34] conducted a study of leaching kinetics of scheelite in hydrochloric acid solution and determined that kinetic model equations are credible and the Avrami equation in Eq. (8) is the best kinetic model equation:

$$\ln[-\ln(1-x)] = \ln k + n \ln t \quad (8)$$

where n is a parameter related to grain properties and grain geometry. When $n \leq 1$, leaching reaction belongs to the type with a maximum initial reaction rate but a decreasing reaction rate over time. When $n=1$, leaching reaction is controlled by chemical reaction, when $n < 0.5$, leaching is controlled by diffusion, and when $0.5 \leq n < 1$, leaching is controlled by chemical reaction and diffusion mixing [31].

Considering the fact that the unreacted shrinking core model's prerequisites require the reacted solid particles to be a single-size compact spherical and have the same chemical properties in all directions [35], combined with the previous SEM analysis, the MPr has more surface pores and gullies. Therefore, it may be more appropriate to use the Avrami equation to describe the reaction process. The fitting results are shown in Fig. 9 and Table 2.

As shown in Fig. 9, an excellent linear fitting relationship at all temperatures, and the correlation coefficient (R^2) shown in Table 2 is not lower than 0.9870, which is much better than the correlation coefficient of the previous model fitting, indicating that the leaching process conforms to the Avrami equation. According to Fig. 9(a), the value of n under the conventional condition at each

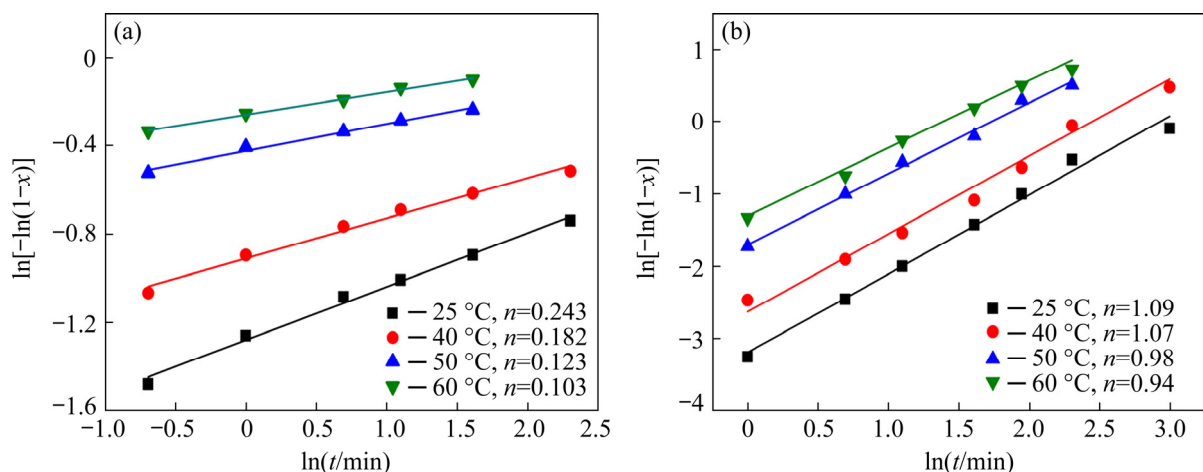
**Fig. 9** Kinetic fitting curves of $\ln[-\ln(1-x)]$ versus $\ln t$ at different temperatures under conventional (a) and ultrasonic (b) conditions

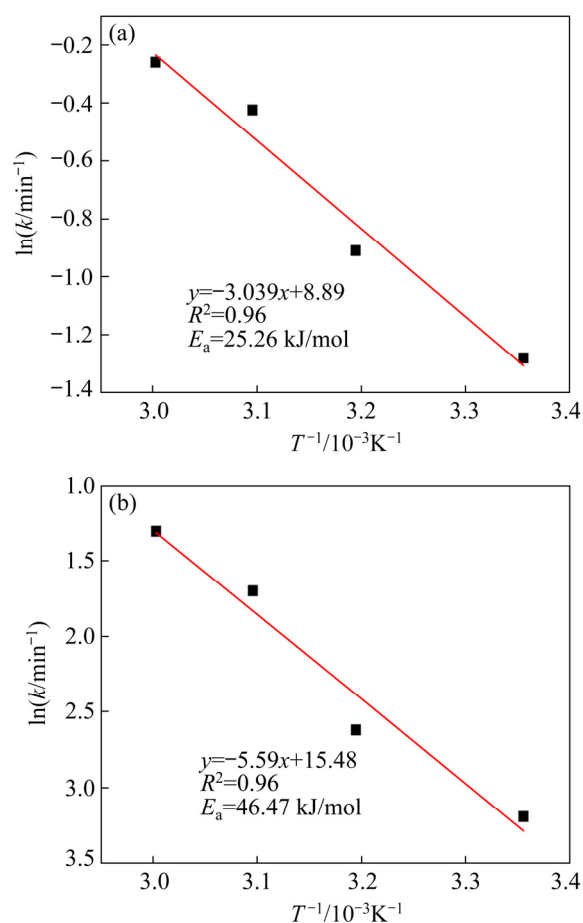
Table 2 Fitting regression equation and correlation coefficient (R^2) of Avrami model at different temperatures under normal leaching

Reaction condition	Temperature/ $^{\circ}\text{C}$	Regression equation	Correlation coefficient, R^2
Conventional	25	$\ln[-\ln(1-x)] = -1.2807 + 0.243 \ln t$	0.9922
	40	$\ln[-\ln(1-x)] = -0.9097 + 0.182 \ln t$	0.9876
	50	$\ln[-\ln(1-x)] = -0.4247 + 0.123 \ln t$	0.9870
	60	$\ln[-\ln(1-x)] = -0.2602 + 0.103 \ln t$	0.9951
Ultrasonic	25	$\ln[-\ln(1-x)] = 3.1919 + 1.090 \ln t$	0.9904
	40	$\ln[-\ln(1-x)] = -2.6217 + 1.073 \ln t$	0.9832
	50	$\ln[-\ln(1-x)] = 1.6998 + 0.981 \ln t$	0.9932
	60	$\ln[-\ln(1-x)] = 1.3022 + 0.939 \ln t$	0.9956

temperature is less than 0.5, indicating that the reaction process is controlled by diffusion and has a large initial reaction rate. While under the ultrasonic condition, the average value of n is 1.02 (Fig. 9(b)), which is approximately equal to 1, indicating that the reaction process is controlled by chemical reaction and diffusion is no longer the primary resistance.

The apparent activation energy E_a and frequency factor A of the reaction can be calculated according to Arrhenius equation [36]. The results are shown in Fig. 10. It can be calculated that the apparent activation energy under the conventional leaching condition is 25.26 kJ/mol, indicating that the reaction process is controlled by solid film diffusion [15,37,38]. The result is consistent with the analysis result according to n value in the Avrami model (Fig. 9), and the value of $\ln A_1$ is 8.89. At the same time, it can be seen the apparent activation energy is 46.47 kJ/mol in the presence of ultrasonic, indicating that the reaction process is controlled by chemical reaction [33,39], which is consistent with the above analysis results based on the average value of n , and the value of $\ln A_2$ is 15.58.

Frequency factor under ultrasonic condition (A_2) is higher than that under conventional condition. The relationship between the two factors is as follows: $A_2/A_1=804$. According to the absolute rate theory, the frequency factor is related to the vibration of molecules participating in the reaction. Under ultrasonic action, the reaction molecules reciprocate along with the ultrasonic, which dramatically accelerates the vibration between molecules and improves the reaction rate, which is difficult to achieve with ordinary mechanical agitation.

**Fig. 10** Relationship between $\ln k$ and $1/T$ of reaction: (a) Conventional condition; (b) Ultrasonic condition

3.5 Mechanism of enhancement in MPr under ultrasonic-assistance

The mechanism for ultrasonic-enhanced selective sulfide precipitation of copper ions can be schematically illustrated in Fig. 11. Under conventional condition, temperature is an important factor affecting the decomposition of MPr at a certain acidity, which will further affect the removal rate of copper ions. At relatively low temperatures,

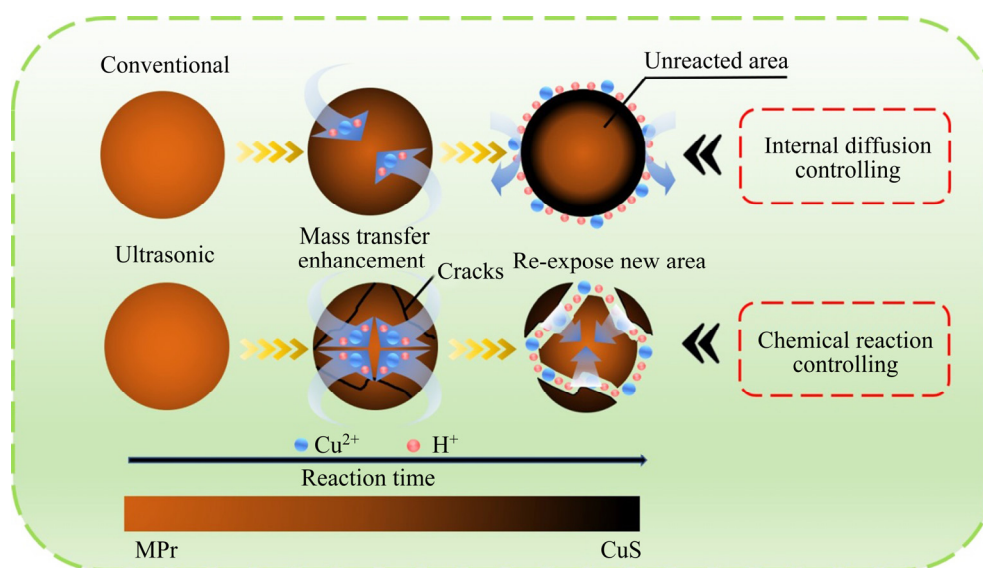


Fig. 11 Mechanism diagram of enhancement in MPr under ultrasonic-assist

the decomposition rate of MPr is slow, and the slowly generated sulfide ions will preferentially react with copper ions to form copper sulfide and coat on the surface of MPr, making the reaction difficult to continue. Such a process can be described as follows: H^+ and Cu^{2+} in the solution diffuse through the reacting solid particles' pores and cracks. At the same time, H^+ reacts with the surface of particles to promote the decomposition of MPr, and S^{2-} produced by MPr decomposition reacts with Cu^{2+} in the solution to form CuS covering the surface of the reaction particles and the inner surface of the pores, which prevent further reactions. At this point, the pore diffusion resistance and the solid layer diffusion resistance become the main resistance. The reaction begins to be controlled by the CuS solid phase film diffusion. The next reaction will proceed in a narrow area between the completely reacted part and the unreacted part. This process is similar to the diffusion control of the unreacted shrinking core model of non-porous solids.

With the introduction of ultrasonic in the system, the CuS solid film originally covered by particles is peeled off under the action of micro-jet and other mechanical effects caused by ultrasonic, and the particles are exposed to the fresh surface again [40]. MPr can be decomposed slowly with the assistance of ultrasonic to release S^{2-} and react with copper ions to generate copper sulfide, which can be proved from the leaching kinetics of iron ions and copper ions removal. In addition, the copper

sulfide products are also easily filtered. Therefore, the introduction of ultrasonic provides the possibility of homogeneous precipitation of copper sulfide from the kinetics. Besides, the CuS flocculent particles are dotted and loosely distributed around and on the surface of the MPr particles due to the vibration and dispersion of ultrasonic waves during the formation process. These effects make it difficult to aggregate into a deep coating on the MPr surface. The reaction-controlled type changes from the previous solid phase film diffusion control to the chemical reaction control. Also, mechanical effects such as micro-jets and acoustic impulse caused by ultrasonic cavitation can promote the macroscopic turbulence of the solution, accelerate the transfer of substances and increase the collision probability of particles, therefore making the solution continuously contact the new solid surface. As a result, the reaction efficiency and utilization rate of MPr are greatly improved.

3.6 Application of MPr in actual leaching solution under ultrasonic-assistance

To investigate the performance of MPr with ultrasonic in the complex leaching solution, the MPr was used for cascade separation of copper and arsenic from the leaching solution of copper soot. The copper removal experiments were conducted at different dosages according to molar ratios of sulfide to copper ions (2, 2.1, 2.3, 2.5, 2.8) at a temperature of 40 °C, ultrasonic power of 90 W,

and reaction time of 30 min. The results are shown in Fig. 12(a). When the molar ratio is 2.5, the removal rate of copper ions has reached 99.4%, and the contents of copper and arsenic in the reaction products are 43.38% and 1.2%, respectively. The separation effect of copper and arsenic is ideal, and the copper product can be set as secondary raw materials to the copper metallurgy process.

The arsenic removal experiments were conducted in the solution after copper removal with different dosages of MPr. The results are presented in Fig. 12(b). It can be found that arsenic removal rate increased from 65.3% to 97% as the dosage of MPr increased from 2.0 to 3.0. The arsenic content

in the product increased first and then decreased with increasing the dosage and reach a maximum of 24.64% when the dosage is 2.8. At this time, the arsenic removal in the solution is 95.2%. Iron content in the solution and product after the separation of copper and arsenic and arsenic removal rate can be seen in Fig. S8 in SI. Overall, the whole process of the copper and arsenic removal with MPr under ultrasonic achieved the ideal results.

Based on the experimental results discussed above, we proposed an environmental and clean process for comprehensive utilization and treatment of copper smelting dust, as shown in Fig. 13. The

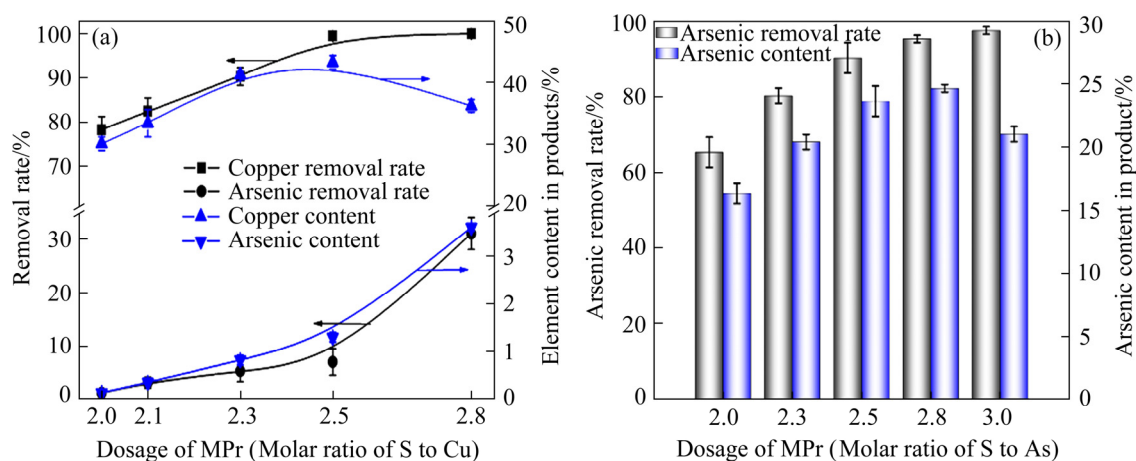


Fig. 12 Effect of MPr dosage on separation of copper and arsenic (a) and arsenic removal rate and arsenic content in product (b)

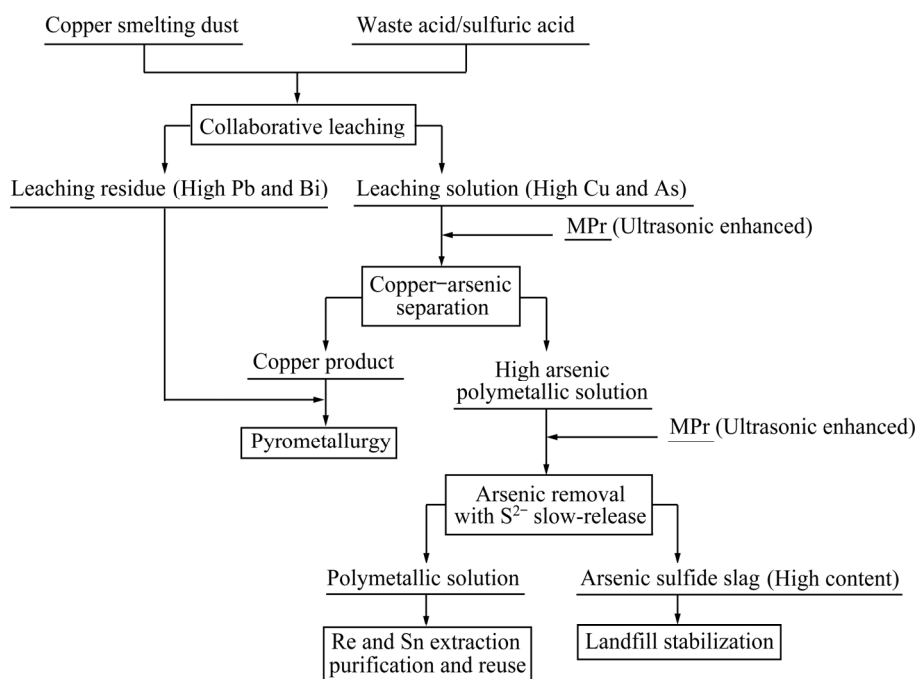


Fig. 13 Technological scheme for comprehensive utilization of copper smelting dust

process consists of two parts: one is the selective collaborative leaching, the other is the highly efficient separation and recovery of copper and arsenic in the leaching solution. The leaching residue and copper separation residue contain high-grade valuable metals, which can be used as raw materials to return to the pyrometallurgy system. The arsenic in the solution is precipitated in the form of arsenic sulfide with high content using MPr. Finally, the wastewater could be used to extract rare metals and reused after purification. The whole scheme achieves highly efficient and environmental disposal of copper smelting dust, which can be used for reference to treating other similar smelting dust.

4 Conclusions

(1) Copper ion removal rate can reach 85.3% at temperature of 25 °C, H₂SO₄ concentration of 50 g/L, MPr dosage of 2, reaction time of 30 min, and ultrasonic power of 60 W. Ultrasound-assistance significantly reduces the acidity and temperature required for the reaction and saves energy consumption.

(2) The remarkable achievements are made by ultrasonic due to its physical and chemical effects in the solution. Ultrasonic treatment can peel off the solid layer (CuS) coating on the surface of MPr and allow the MPr to expose the fresh surface again, thus prompting the reaction to proceed further. In addition, the strong vibration caused by ultrasonic causes large cracks on the particle surface and enhances the mass transfer at the liquid–solid interface.

(3) The kinetic results show that the reaction control type changes from diffusion control to chemical reaction control under ultrasonic conditions, and the apparent activation energies are 25.26 and 46.47 kJ/mol, respectively. The diffusion being no longer the primary resistance means that the generated CuS seldom coats on the surface.

(4) The experimental results in the actual system of dust leaching solution displayed that by controlling the dosage of MPr, copper products with grade of 43.38% and 24.64% arsenic products were obtained, respectively. Although a large number of iron ions finally enter the solution, well-established technologies such as extraction or goethite can be

used to achieve iron separation.

Acknowledgments

This work was financially supported by the National Key Scientific Research Project, China (Nos. 2018YFC1901601, 2018YFC1901602), the Fundamental Research Funds for the Central Universities of Central South University, China (No. 2021zzts0307), the National Natural Science Foundation of China (No. 51804340), the Innovation-driven Plan of Central South University, China (No. 2018CX036), the Collaborative Innovation Center for Clean and Efficient Utilization of Strategic Metal Mineral Resources, China, and Key Laboratory of Hunan Province for Clean and Efficient Utilization of Strategic Calcium-containing Mineral Resources, China (No. 2018TP1002).

Supplementary information

The supplementary information (Tables S₁–S₃ and Figs. S₁–S₈) in this work can be found at: <http://www.yxycn.com/download/TNMSC-202202-24-file.pdf>.

References

- [1] KE J J, QIU R Y, CHEN C Y. Recovery of metal values from copper smelter flue dust [J]. *Hydrometallurgy*, 1984, 12(2): 217–224.
- [2] MONTENEGRO V, SANO H, FUJISAWA T. Recirculation of high arsenic content copper smelting dust to smelting and converting processes [J]. *Minerals Engineering*, 2013, 49: 184–189.
- [3] GUO L, LAN J R, DU Y G, ZHANG T C, DU D Y. Microwave-enhanced selective leaching of arsenic from copper smelting flue dusts [J]. *Journal of Hazardous Materials*, 2020, 386: 121964.
- [4] SHIBASAKI T, HASEGAWA N. Combined hydro-metallurgical treatment of copper smelter dust and lead smelter copper dross [J]. *Hydrometallurgy*, 1992, 30(1–3): 45–57.
- [5] SHIBAYAMA A, TAKASAKI Y, WILLIAM T, YAMATODANI A, HIGUCHI Y, SUNAGAWA S, ONO E. Treatment of smelting residue for arsenic removal and recovery of copper using pyro-hydrometallurgical process [J]. *Journal of Hazardous Materials*, 2010, 181(1–3): 1016–1023.
- [6] KUCHAR D, FUKUTA T, ONYANGO M S, MATSUDA H. Sulfidation treatment of molten incineration fly ashes with Na₂S for zinc, lead and copper resource recovery [J]. *Chemosphere*, 2007, 67(8): 1518–1525.
- [7] ZHANG X F, TIAN J, HU Y H, HAN H S, LUO X P, SUN W, YUE T, WANG L, CAO X F, ZHOU H P. Selective

- sulfide precipitation of copper ions from arsenic wastewater using monoclinic pyrrhotite [J]. *Science of the Total Environment*, 2020, 705: 135816.
- [8] YANG Y, CHEN T H, LI P, XIE Q Q, ZHAN X M. Cu removal from acid mine drainage by modified pyrite: Batch and column experiments [J]. *Mine Water and the Environment*, 2017, 36(3): 371–378.
- [9] LI L, ZHAI L Y, ZHANG X X, LU J, CHEN R J, WU F, AMINE K. Recovery of valuable metals from spent lithium-ion batteries by ultrasonic-assisted leaching process [J]. *Journal of Power Sources*, 2014, 262: 380–385.
- [10] YAN J W, PAN D A, LI B. Application of ultrasonic intensification in hydrometallurgy leaching process [J]. *The Chinese Journal of Process Engineering*, 2020, 20(11): 1241–1247. (in Chinese)
- [11] GÜNGÖR H, ELIK A. Comparison of ultrasound-assisted leaching with conventional and acid bomb digestion for determination of metals in sediment samples [J]. *Microchemical Journal*, 2007, 86(1): 65–70.
- [12] XIE F C, LI H Y, MA Y, LI C C, CAI T T, HUANG Z Y, YUAN G Q. The ultrasonically assisted metals recovery treatment of printed circuit board waste sludge by leaching separation [J]. *Journal of Hazardous Materials*, 2009, 170(1): 430–435.
- [13] ZHANG L B, GUO W Q, PENG J H, LI J, LIN G, YU X. Comparison of ultrasonic-assisted and regular leaching of germanium from by-product of zinc metallurgy [J]. *Ultrasonics Sonochemistry*, 2016, 31: 143–149.
- [14] BRUNELLI K, DABALÀ M. Ultrasound effects on zinc recovery from EAF dust by sulfuric acid leaching [J]. *International Journal of Minerals, Metallurgy, and Materials*, 2015, 22(4): 353–362.
- [15] LI H Y, LI S W, PENG J H, SRINIVASAKANNAN C, ZHANG L B, YIN S H. Ultrasound augmented leaching of nickel sulfate in sulfuric acid and hydrogen peroxide media [J]. *Ultrasonics Sonochemistry*, 2018, 40: 1021–1030.
- [16] ZHANG K H, LI B, WU Y F, WANG W, LI R B, ZHANG Y N, ZUO T Y. Recycling of indium from waste LCD: A promising non-crushing leaching with the aid of ultrasonic wave [J]. *Waste Management*, 2017, 64: 236–243.
- [17] ZHANG X F, LIU S M, CAO X F, HAN H S, SUN W, CHENG P F, WANG L. Arsenic removal technology based on mechanical activation of natural pyrrhotite [J]. *Journal of Central South University (Science and Technology)*, 2019, 50(11): 2623–2632. (in Chinese)
- [18] JANA A, JANA S K, SARKAR D, AHUJA T, BASURI P, MONDAL B, BOSE S, GHOSH J, PRADEEP T. Electrospray deposition-induced ambient phase transition in copper sulphide nanostructures [J]. *Journal of Materials Chemistry A*, 2019, 7(11): 6387–6394.
- [19] GOH S W, BUCKLEY A N, LAMB R N, ROSENBERG R A, MORAN D M. The oxidation states of copper and iron in mineral sulfides, and the oxides formed on initial exposure of chalcopyrite and bornite to air [J]. *Geochimica et Cosmochimica Acta*, 2006, 70(9): 2210–2228.
- [20] YANG C R, JIAO F, QIN W Q. Cu-state evolution during leaching of bornite at 50 °C [J]. *Transactions of Nonferrous Metals Society of China*, 2018, 28(8): 1632–1639.
- [21] KLAUBER C, PARKER A, van BRONSWIJK W, WATLING H. Sulphur speciation of leached chalcopyrite surfaces as determined by X-ray photoelectron spectroscopy [J]. *International Journal of Mineral Processing*, 2001, 62(1–4): 65–94.
- [22] GHAHREMANINEZHAD A, DIXON D G, ASSELIN E. Electrochemical and XPS analysis of chalcopyrite (CuFeS₂) dissolution in sulfuric acid solution [J]. *Electrochimica Acta*, 2013, 87: 97–112.
- [23] CHEN B, BAO S X, ZHANG Y M, LI S. A high-efficiency and sustainable leaching process of vanadium from shale in sulfuric acid systems enhanced by ultrasound [J]. *Separation and Purification Technology*, 2020, 240: 116624.
- [24] PICAZO-RODRÍGUEZ N G, de JESUS SORIA-AGUILAR M D, MARTÍNEZ-LUÉVANOS A, ALMAGUER-GUZMÁN I, CHAIDEZ-FÉLIX J, CARRILLO-PEDROZA F R. Direct acid leaching of sphalerite: An approach comparative and kinetics analysis [J]. *Minerals*, 2020, 10(4): 359.
- [25] WEN C Y. Noncatalytic heterogeneous solid-fluid reaction models [J]. *Industrial & Engineering Chemistry*, 1968, 60(9): 34–54.
- [26] ELÇIÇEK H, KOÇAKERIM M M. Leaching kinetics of ulexite ore in aqueous medium at different CO₂ partial pressures [J]. *Brazilian Journal of Chemical Engineering*, 2018, 35(1): 111–122.
- [27] AVRAMI M. Kinetics of phase change. I: general theory [J]. *The Journal of Chemical Physics*, 1939, 7(12): 1103–1112.
- [28] WILKINSON A P, SPECK J S, CHEETHAM A K, NATARAJAN S, THOMAS J M. In situ X-ray diffraction study of crystallization kinetics in PbZr_{1-x}Ti_xO₃ (PZT, x=0.0, 0.55, 1.0) [J]. *Chemistry of Materials*, 1994, 6(6): 750–754.
- [29] FARJAS J, ROURA P. Modification of the Kolmogorov–Johnson–Mehl–Avrami rate equation for non-isothermal experiments and its analytical solution [J]. *Acta Materialia*, 2006, 54(20): 5573–5579.
- [30] KHAWAM A, FLANAGAN D R. Solid-state kinetic models: Basics and mathematical fundamentals [J]. *Journal of Physical Chemistry B*, 2006, 110(35): 17315–17328.
- [31] LI Q C, LIU Z Y, LIU Q Y. Kinetics of vanadium leaching from a spent industrial V₂O₅/TiO₂ catalyst by sulfuric acid [J]. *Industrial & Engineering Chemistry Research*, 2014, 53(8): 2956–2962.
- [32] TIAN J, ZHANG X F, WANG Y F, HAN H S, SUN W, YUE T, SUN J T. Alkali circulating leaching of arsenic from copper smelter dust based on arsenic–alkali efficient separation [J]. *Journal of Environmental Management*, 2021, 287: 112348.
- [33] HE G X, ZHAO Z W, WANG X B, LI J T, CHEN X Y, HE L H, LIU X H. Leaching kinetics of scheelite in hydrochloric acid solution containing hydrogen peroxide as complexing agent [J]. *Hydrometallurgy*, 2014, 144/145: 140–147.
- [34] SHI M Q, MIN X B, SHEN C, CHAI L Y, KE Y, YAN X, LIANG Y J. Separation and recovery of copper in Cu–As-bearing copper electrorefining black slime by oxidation acid leaching and sulfide precipitation [J]. *Transactions of Nonferrous Metals Society of China*, 2021, 31(4): 1103–1112.
- [35] LI J T, ZHAO Z W, DING W T. Kinetics of scheelite concentrate leached by sodium phosphate under ultrasound

- [J]. Chinese Journal of Nonferrous Metals, 2014, 24: 1607–1615. (in Chinese)
- [36] OUDENNE P D, OLSON F A. Leaching kinetics of malachite in ammonium carbonate solutions [J]. Metallurgical Transactions B, 1983, 14(1): 33–40.
- [37] LIU W, TANG M T, TANG C B, HE J, YANG S H, YANG J G. Dissolution kinetics of low grade complex copper ore in ammonia–ammonium chloride solution [J]. Transactions of Nonferrous Metals Society of China, 2010, 20(5): 910–917.
- [38] ZHENG Y J, CHEN K K. Leaching kinetics of selenium from selenium–tellurium-rich materials in sodium sulfite solutions [J]. Transactions of Nonferrous Metals Society of China, 2014, 24(2): 536–543.
- [39] ANTONIJEVIĆ M M, PACOVIĆ N V. Investigation of molybdenite oxidation by sodium dichromate [J]. Minerals Engineering, 1992, 5(2): 223–233.
- [40] POKHREL N, VABBINA P K, PALA N. Sonochemistry: Science and engineering [J]. Ultrasonics Sonochemistry, 2016, 29: 104–128.

超声强化单斜磁黄铁矿从铜烟灰中选择性硫化沉淀铜离子

张荣斐^{1,2}, 袁佳^{1,2}, 田佳^{1,2}, 韩海生^{1,2}, 孙伟^{1,2},
岳彤^{1,2}, 杨越^{1,2}, 王丽^{1,2}, 曹学锋^{1,2}, 卢承龙^{1,2}

1. 中南大学 资源加工与生物工程学院, 长沙 410083;
2. 中南大学 战略含钙矿物资源清洁高效利用湖南省重点实验室, 长沙 410083

摘要: 在单斜磁黄铁矿(MPr)处理废水重金属离子过程中表面产生的硫化物钝化膜严重阻碍进一步反应。采用超声波技术辅助 MPr 回收铜离子。XPS 分析结果表明, 反应过程中 MPr 表面存在 CuS 产物。XRD 和 SEM 分析结果表明, 在超声条件下颗粒表面的 CuS 被剥离。动力学结果表明, 常规和超声条件下的反应均符合 Avrami 模型。在超声条件下, 随着固体层的剥离, 反应过程由扩散控制转变为化学反应控制。超声波的存在显著降低反应所需的酸度和温度, 提高 MPr 的利用效率; 通过控制 MPr 的用量, 铜烟灰浸出液中铜和砷的去除率分别达到 99% 和 95%以上。

关键词: 超声辅助处理; 单斜磁黄铁矿; 铜烟灰; 除砷; 选择性硫化沉淀

(Edited by Wei-ping CHEN)